IEEE Access
Multidisciplinary | Rapid Review | Open Access Journal

Received June 6, 2020, accepted June 21, 2020, date of publication July 3, 2020, date of current version September 3, 2020.

Digital Object Identifier 10.1109/ACCESS.2020.3006903

An Improved Salp Swarm Algorithm With Spiral Flight Search for Optimizing Hybrid Active Power Filters' Parameters

LEYINGYUE ZHANG, CHUNQUAN LI, (Member, IEEE), YUFAN WU, JUNRU HUANG, AND ZHILING CUI

School of Information Engineering, Nanchang University, Nanchang 330029, China

Corresponding author: Chunquan Li (lichunquan@ncu.edu.cn)

This work was supported in part by the National Natural Science Foundation of China under Grant 61863028, Grant 61503177, and Grant 81660299, in part by the China Scholarship Council under the State Scholarship Fund under Grant CSC 201606825041, in part by the Science and Technology Department of Jiangxi Province of China under Grant 20161ACB21007, Grant 20171BBE50071, and Grant 20171BAB202033, and in part by the Education Department of Jiangxi province of China under Grant GJJ14228 and Grant GJJ150197.

ABSTRACT In view of various issues occasioned by harmonic pollution in the power system, the optimization of the filter parameters is of great significance. However, under the system constraints, estimating the filter parameters accurately and reliably is a challenging task. To complete this task, this paper proposes an improved salp swarm algorithm based on the spiral flight search strategy (ISSA-SFS), which rationally integrates the spiral flight search (SFS) strategy, the multiple leader (ML) strategy, and the random learning (RL) strategy with two improved evolution phases: the improved lead phase (ILP) and the improved follow phase (IFP). In the ILP, the SFS strategy is introduced to enhance the global search capability and avoid premature convergence. Furthermore, in the ILP, an ML strategy is proposed to select multiple leaders, further strengthening the global search capability of the proposed algorithm. In the IFP, a simple RL strategy is developed to learn two different random individuals, efficiently improving the local exploitation. The proposed algorithm ISSA-SFS is applied to optimize two prominent hybrid active power filter (HAPF) topologies, and each topology contains four different study cases. The overall experimental results indicate that the ISSA-SFS is a more promising alternative to achieve the optimal design of HAPFs compared with other well-established algorithms, especially in terms of accuracy and robustness.

INDEX TERMS Parameter optimization, harmonic pollution (HP), hybrid active power filter (HAPF), salp swarm algorithm (SSA), spiral flight search (SFS).

I. INTRODUCTION

With the rapid development of electronics industry technologies, there are more and more non-linear loads in the modern power system, which might lead to significant line voltage distortion [1]. The voltage distortion is the primary source of harmonic pollution, and harmonic pollution would influence power quality significantly and endanger the safety of the power grid and power equipment. Therefore, the monitoring and reduction of harmonic pollution have become important research topics [2].

Existing schemes for controlling harmonic pollution include two categories. One is to modify the characteristics of non-linear loads in power electronic devices to correct the power factor, while this approach has the disadvantages of high cost and low efficiency. The other is to install passive filters, active filters, or hybrid active filters to compensate reactive power [3]–[5]. Due to the technical or economic defects of passive or active filters [6], the combination of passive and active topology is usually employed to control harmonic, which is called the hybrid active power filter (HAPF). HAPF is more stable and has a lower cost than passive power filter (PPF) and active power filter (APF) because the hybrid topology combines and utilizes the advantages of PPF and APF. Consequently, the harmonic problem can be solved as much as possible by HAPF, and the application of HAPF is a promising approach for reducing harmonics [7].

So far, the research on HAPF is mainly about the design of different topologies [8]–[10], while parameter optimization of HAPFs is relatively few. One possible reason is that

The associate editor coordinating the review of this manuscript and approving it for publication was Amir Masoud Rahmani.

research in this area is relatively challenging. In HAPF, the main challenge is how to choose the appropriate APF gain, passive inductance and capacitance response values, while satisfying the system's constraints on single and overall voltage and current harmonic distortion levels [11]. In this case, it becomes particularly important to develop a technical solution that effectively optimizes the parameters of the HAPF.

The optimization issue of HAPF parameters in power systems can come down to a single objective constrained optimization issue. To be more specific, the target of the function is to reach a compromise solution based on some conditions. Due to the nonlinearity of the loads, it is difficult to find a satisfactory solution by conventional methods. Compared with the traditional gradient-based method, meta-heuristic methods are insensitive to the initial condition of solutions and have higher efficiency [12], [13]. So that meta-heuristic methods are of general technical significance, and they have become a powerful choice for solving many practical engineering problems [14]. For instance, Ochoa *et al.* [15] used the fuzzy differential evolution (FDE) algorithm in the optimization of fuzzy controller design. Castillo *et al.* [16] applied the Karnik and Mendel algorithm for the defuzzification process and presented a comparative study. In [17], a multiple learning backtracking search algorithm (MLBSA) is proposed for the parameter identification issues of photovoltaic models, etc. Nevertheless, in previous studies, the number of references using heuristic optimization techniques to extract parameters of the HAPF is limited. In 2017, Biswas *et al.* [11] applied a meta-heuristic algorithm based on the success-history based parameter adaptation for differential evolution (SHADE) algorithm called L-SHADE to optimize appropriate parameters of two prominent HAPF structural configurations. The L-SHADE algorithm improved the performance of SHADE by adopting a linear population size reduction (LPSR) strategy, and this meta-heuristic method exhibited the best performance among all non-hybrid algorithms in the CEC 2014 competition on single objective real-parameter optimization [11]. Therefore, L-SHADE is useful for the HAPF parameter design issue, and it has a competitive filtering effect. However, the performance of L-SHADE still has the potential to improve. Therefore, developing a competitive meta-heuristic algorithm to find a more accurate and reliable solution is still a challenging task.

Salp swarm algorithm (SSA) is a young and popular meta-heuristic algorithm proposed by Mirjalili *et al.* in 2017 [18]. The algorithm is inspired by the swarming behavior of salps. Similar to most meta-heuristic algorithms, SSA is optimized from a set of multiple solutions with randomly given positions, then these solutions are adjusted through the iterative process. Research points out that within a certain operating time [19], SSA has a better capability to seek out the global solution, and the parameter tuning is less than other meta-heuristic algorithms, such as simulated annealing (SA) [20], hill-climbing [21], and grey wolf optimization (GWO) [22]. Furthermore, SSA holds the advantages of simplicity and ease of hybridization. In summary, SSA has certain strengths among the above algorithms. Therefore, SSA has been widely used in engineering applications [23], machine learning [24], image processing [25], and many other application fields [26], [27]. In SSA, the population consists of a leader and followers. The update process of salps includes two different continuous phases: the lead phase (LP) and the follow phase (FP). The former represents the leader's moving stage, while the latter represents the moving stage of followers. To the best of our knowledge, the SSA has renewed for diverse variants to solve different optimization problems. The main variants of SSA can be divided into two categories: hybridization of SSA and modifications of SSA [27]. The hybrid SSA variants are generally formed by mixing SSA with another algorithm or technical methods. For example, Singh *et al.* [29] developed a new algorithm called HSSASCA by combining SSA with a sine cosine algorithm (SCA), the performance of HSSASCA is verified in twenty-two standard functions. Asaithambi and Rajappa [23] designed a hybrid algorithm based on SSA and Hooke-Jeeves algorithm called SSA-HJ, which is applied for optimizing the sizing of a CMOS differential amplifier and the comparator circuit. As for modified SSA variants, most of them modify the original SSA by adopting different strategies in the above two continuous phases, i.e., LP and FP. For instance, an improved salp swarm algorithm (ISSA) is proposed in [29] by introducing an inertia weight into LP and FP as a control parameter, which speeds up the convergence and achieves better performance. Sayed *et al.* proposed a new algorithm in [30], the algorithm only modified LP while FP followed the original version, the amended LP introduced the chaotic theory, which significantly improves the exploration capability. In [31], Qais *et al.* presented an enhanced salp swarm algorithm (ESSA) to improve the basic SSA. According to the Gaussian model, the covariance variable in LP increased its step size in the exponential direction, and the space equation in FP is modified by replacing the constant with a random number.

Although SSA and its variant algorithms have some advantages, like other meta-heuristic algorithms, they still have some imperfections. For example, the basic SSA may be trapped in the stagnation point [19], which results in local optimization and slow convergence speed. As for variants of SSA, some of them succeed in avoiding falling into local optimal and accelerating the convergence speed. In spite of this, no free lunch (NFL) [32] proves that each meta-heuristic algorithm has different characteristics, so each algorithm cannot deal with all optimization problems. To the best of our knowledge, so far, there are no attempts of using SSA method in exacting the parameters of the two HAPF topologies. In this case, we develop an improved salp swarm algorithm based on spiral flight search strategy (ISSA-SFS) and apply it for extracting the optimal HAPF parameters.

In ISSA-SFS, inspired by reference [33], we first adopt the spiral flight search strategy (SFS) for optimizing the search space and shortening the distance between leaders

and the food source. Furthermore, in order to obtain better performance in terms of achieving an optimal global solution, we propose a multiple leader (ML) strategy which expands the leader group from one leader to multiple leaders. In this way, more than one leader update towards food, and the single-chain structure is modified to a multi-chain structure. As a further step, we further develop a random learning (RL) strategy for enhancing the population diversity and accelerate the convergence speed. The updated trajectory of the follower group is modified to update based on two individuals randomly selected, instead of moving the follower's position based on the previous one. In order to achieve a good balance between the global and local search capabilities of the algorithm, we integrate the above strategies into the ILP and IFP of ISSA-SFS. To assess the performance of ISSA-SFS, we execute some comparisons between it and six well-established algorithms on extracting appropriate parameters of two commonly used HAPF topologies. The comparative results indicate that the performance of ISSA-SFS is superior to the original SSA algorithm and other popular heuristic algorithms: L-SHADE [11], moth-flame optimization algorithm (MFO) [33], particle swarm optimization (PSO) [34], teaching-learning based optimization algorithm (TLBO) [35], and multi-verse optimizer (MVO) [36].

The main contributions of this paper are described as follows:

1) We propose a new ISSA-SFS algorithm, which rationally combines the spiral flight search (SFS) strategy, the multiple leader (ML) strategy, and the random learning (RL) strategy with two improved evolution phases: the improved lead phase (ILP) and the improved follow phase (IFP). These strategies can effectively balance the exploitation and exploration performance in the entire iteration progress. The effectiveness of ISSA-SFS is extensively evaluated on two popular HAPF topologies to extract the corresponding parameters effectively.

2) In the ILP, the spiral flight search (SFS) strategy is introduced to enhance the global search capability and avoid premature convergence, because the SFS strategy can enable salps to move spirally towards the food target to update their positions in the iterative process. Furthermore, in the ILP, different from the original SSA that uses a leader, the proposed ISSA-SFS adopts a multiple leader (ML) strategy that selects multiple leaders by the sorting mechanism to approach the food source, which can further strengthen the global search capability of the proposed algorithm.

3) In the IFP, a simple random learning (RL) strategy is developed by enabling each follower to learn two different random individuals instead of the previous individual from the sorting mechanism [18], which can efficiently improve the local exploitation and accelerate the convergence speed to the global optimum solution.

4) The proposed ISSA-SFS is used for the parameter extraction issue of two typical HAPF topologies. Further, the ISSA-SFS algorithm is compared with other well-established algorithms, which indicates that ISSA-SFS is a promising alternative to parameter optimization issues of HAPF.

The remainder of this paper is structured as follows: Section II illustrates the HAPF configurations and the objective function. Section III introduces a brief introduction to metaheuristic algorithms, the original SSA algorithm, and the spiral flight search strategy. Section IV provides a detailed description of the proposed algorithm ISSA-SFS. The experimental results and discussion are given in Section V. Eventually, Section VI summarizes the paper and concludes the work.

II. RELATED WORK OF HAPF TOPOLOGIES

Passive power filter (PPF) is a kind of filtering equipment mainly made up of one or more sets of single-tuned filters. Specifically, it is a circuit wiring combination of a filter capacitor, reactor, and resistor, so it is also known as the LC filter. As is well-known, some drawbacks exist in the passive filter, so the conventional PPF often connects to the harmonic source in parallel to provide an effective solution. Another kind of power electronic equipment active power filter (APF) is also applied to eliminate grid harmonics. It consists of a pulse width modulation (PWM) inverter, which is mainly composed of giant transistors (GTR) [37]. The APF can achieve most functions of PPF in terms of technical requirements.

As mentioned before, passive filters usually connect in parallel with harmonic sources or loads in the circuit. Besides, recent studies suggest that compared with traditional passive filters, the use of parallel passive filters is more extensive. The primary purpose of designing the parallel passive filters is to reduce the harmonic current injected into the power supply, and the performance of power systems can be improved by suppressing harmonics [38]. This structure provides a low-impedance parallel circuit for the harmonic current generated by the load [39]. As for the active filter, it also includes the series APF and the parallel APF [40]. The series APF connects in series with loads through a coupling transformer, while the parallel APF connects to the grid in parallel with the system loads. Similarly, in practical applications, series APFs are not as widely used as parallel APFs, because the former may increase the loss of the line and the circuit is inconvenient to inspect and maintain. In contrast, parallel APFs can not only simply operated but also the number of filters can be controlled according to grid requirements. In this way, the system can obtain sufficient compensation current. However, the parallel APF also has certain limitations, when only using the parallel APF in the power grid, the filter needs a large capacity, and it will also encounter problems, such as complex circuit structure and high operating cost [39].

As discussed above, whether the filter is series or parallel, passive or active, there are still technical problems that cannot be solved. This difficulty makes the research of hybrid active filters more attractive. Generally, a hybrid active filter is a series or parallel connection of two basic passive filters and two basic active filters. Inheriting and combining the

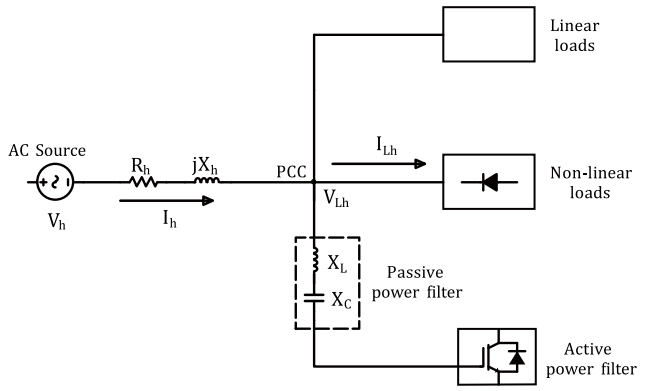

FIGURE 1. Circuit configurations of 'APF in series with shunt passive filter.'

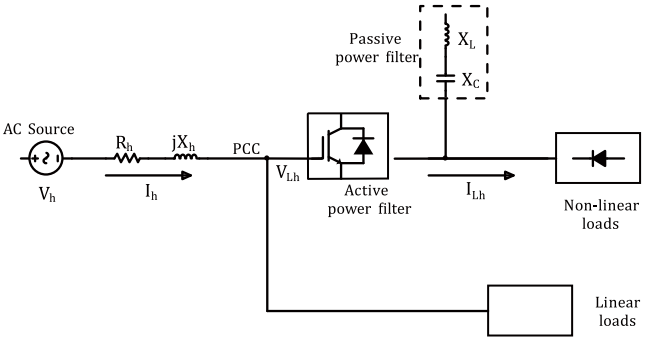

FIGURE 2. Circuit configurations of 'combined series APF and shunt passive filter.'

advantages of PPF and APF will lead to better solutions and more stable performance, which is the significance of HAPF research. In recent research, two topologies with ideal performance are increasingly employed in a power system. They are 'APF in series with shunt passive filter' and 'combined series APF and shunt passive filter', these two types of HAPF structure configurations are commonly applied in practical problem solving and engineering applications. The above two HAPF topologies are respectively illustrated in Figure 1 and Figure 2 without indicating the matching transformers, note that the point of common coupling (PCC) is the join points of the passive filter and other linear loads [11]. In the following, this paper will explore the filtering principle of the two configurations and analyze the connection features of the circuit.

A. APF IN SERIES WITH SHUNT PASSIVE FILTER

As shown in Fig. 1, in this HAPF topology, the filtering system is a series connection of the active filter and passive filters, and the system connects in parallel with loads. The passive filter in this topology is a parallel passive filter, also a single tuned passive filter combined with its inductance X_L and capacitive reactance X_C. The basic principle of APF is to inject the compensation current generated by the compensation device into the grid. When the compensation current is equal to the harmonic current of the compensated object but flows in the opposite direction, the harmonic current in the power grid can be eliminated, only the fundamental wave of the power system remains. In this structure, the APF forces all harmonic currents from the load to the parallel PPF, in this way, not only the load harmonic current is compensated, but also no amplified harmonic current flows in the source. As a result, the compensation performance of passive components is improved. At the same time, the active filter will provide the fundamental currency of the system, and then the line voltage is applied to the PPF, which means that the rated voltage required for the active filter will be significantly reduced [41].

The single-phase equivalent circuit at the fundamental frequency of this HAPF topology indicates in Fig. 3 [11]. In Fig. 3, the parameter value at the fundamental frequency takes the index h equal to '1'. At harmonic frequencies, the single-phase equivalent circuit of the first configuration shows in figure 4.

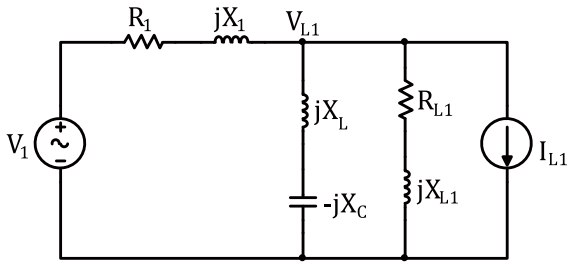

FIGURE 3. Single-phase equivalent circuit at the fundamental frequency.

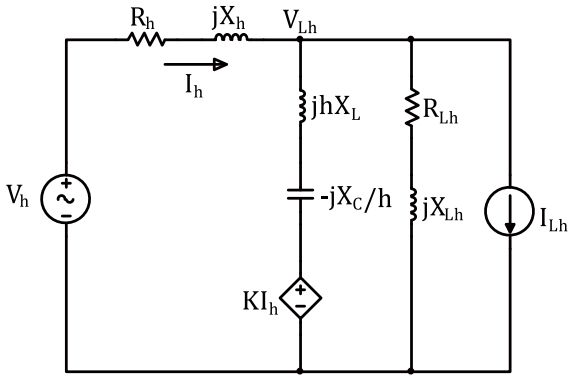

FIGURE 4. Single-phase equivalent circuit for config.1 'APF in series with shunt passive filter' at harmonic frequencies.

Assume that a non-linear load appears as a voltage source, the voltage of the load can be counted into V_{Lh}, and when the non-linear load appears as a current source, the load's current can be represented by I_{Lh}. It can be seen that the load harmonic source in this topology behaves as a current source, so it is called a current-source non-linear load. The current flowing through the load is accounted in I_{Lh} and the voltage across the load is accounted in V_{Lh}, where the subscript h is the order of harmonics. Additionally, V_h and I_h stand for harmonic voltage and current of non-linear power supply, respectively. The active power filter in this topology operates as a controlled voltage source V_{AF} which applies a voltage signal to its terminal, the applied voltage signal equals to

K times as large as the harmonic component of the system supply current, i.e. $V_{AF} = KI_h$. The proportionality constant 'K' denotes the filter gain that exists only at harmonic frequencies, the gain of the filter plays an important role as a harmonic resistance.

Inspired by reference [42], the Thevenin voltage source representing the utility supply voltage and the harmonic current source representing the non-linear load are:

$$v(t) = \sum_h v_h(t) \tag{1}$$

$$i_L(t) = \sum_h i_{Lh}(t) \tag{2}$$

R_h, X_h and Z_h denote the transmission system resistance, inductive reactance, and impedance at h-th harmonic. The relationship between the three parameters can be indicated to the following formula:

$$Z_h = R_h + jX_h \tag{3}$$

Similarly, R_{Lh}, X_{Lh} and Z_{Lh} represent the non-linear load resistance, inductive reactance, and impedance at h-th harmonic. G_{Lh}, B_{Lh} and Y_{Lh} represent the non-linear load conductance, susceptance, and admittance at h-th harmonic. The equivalent load impedance and admittance can be expressed as below, respectively:

$$Z_{Lh} = R_{Lh} + jX_{Lh} \tag{4}$$

$$Y_{Lh} = G_{Lh} - jB_{Lh} \tag{5}$$

From the equivalent circuit for config.1 'APF in series with shunt passive filter', the compensated utility supply current I_h and the compensated load voltage V_{Lh} can be acquired via equations (6) and (7):

$$I_h = \frac{A + jB}{C + jD} \tag{6}$$

$$V_{Lh} = \frac{E + jF}{C + jD} \tag{7}$$

where we can observe that the equations introduce some intermediate variable as follows:

$$X_{Ph} = hX_L - \frac{X_C}{h} \tag{8}$$

$$A = V_h R_{Lh} - I_{Lh} X_{Lh} X_{Ph} \tag{9}$$

$$B = V_h(X_{Lh} + X_{Ph}) + I_{Lh} R_{Lh} X_{Ph} \tag{10}$$

$$C = R_h R_{Lh} - X_h X_{Lh} + KR_{Lh} - (X_{Lh} + X_h) X_{Ph} \tag{11}$$

$$D = R_{Lh} X_h + R_h X_{Lh} + KX_{Lh} - (R_{Lh} + R_h) X_{Ph} \tag{12}$$

$$E = V_h(KR_{Lh} - X_{Lh} X_{Ph}) + I_{Lh}(R_{Lh} X_h + R_h X_{Lh}) X_{Ph} \tag{13}$$

$$F = V_h(KX_{Lh} + R_{Lh} X_{Ph}) - I_{Lh}(R_h R_{Lh} - X_h X_{Lh}) X_{Ph} \tag{14}$$

B. COMBINED SERIES APF AND SHUNT PASSIVE FILTER

Fig. 2 indicates the second discussed HAPF topology, in which the active filter is coupled in the system through an interface transformer and connected in series with the non-linear load in the grid, the passive filter in the circuit is connected in parallel across the load. From Fig. 2, the passive filter of this topology is a shunt passive filter cascaded an inductor X_L and a capacitive reactance X_C, it is in common with the passive filter of the first topology. Furthermore, the active filter coupled in the power grid is a series active filter.

In order to improve the compensation performance of the system, the series active filter needs to eliminate the influence of resonance and source impedance by providing zero impedance at the fundamental wave and high impedance at the harmonics. Similar to the first topology, the load harmonic current is also absorbed by the parallel passive filter. The series APF is referred to as "harmonic isolator" because the harmonic current between the supply source and loads is isolated by the active filter. As a result, the rating current of this series active filter is much smaller than conventional active filters. This HAPF topology is suitable for improving power quality and eliminating harmonic pollution.

For the fundamental frequency and harmonic frequencies, the single-phase equivalent circuits of this HAPF topology are illustrated in Figures 3 and 5, respectively. The equivalent circuits of the two topological structures under the fundamental wave are identical, and the symbols of circuit parameters are also the same as those in the first HAPF topology. However, due to the different positions of the active filter, the equivalent circuits under harmonics are different, which results in the differences in the filtering principle between the two topologies.

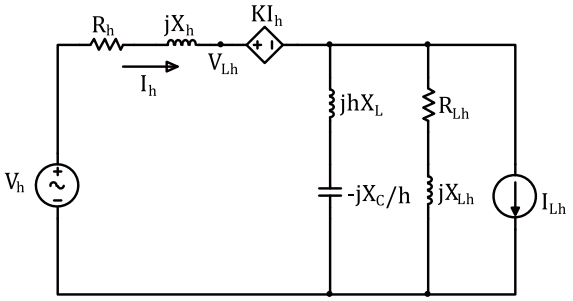

FIGURE 5. Single-phase equivalent circuit for config.2' combined series APF and shunt passive filter' at harmonic frequencies.

According to the equivalent circuit in Fig. 5, the compensated utility supply current I_h for config.2' combined series APF and shunt passive filter' is obtained via formula (15) and the compensated load voltage V_{Lh} is calculated by formula (16).

$$I_h = \frac{A + jB}{C + jD'} \tag{15}$$

$$V_{Lh} = \frac{E + jF'}{C + jD'} \tag{16}$$

Note that A, B, C and D are given in the previous section, so there are another two equations:

$$D' = D + KX_{Ph} \tag{17}$$

$$F' = F + V_h KX_{Ph} \tag{18}$$

C. CONSTRAINTS AND OBJECTIVE FUNCTION FORMULATION

The analysis presented above suggests that HAPF can effectively overcome the obstacles encountered by only using the active filter or the passive filter, and it can achieve voltage control of the power line, thereby verifying the practical feasibility of HAPF topology. Recalling reference [11], the analysis of HAPF topology focuses on optimizing X_L, X_C and K with consideration of non-linear loads and sources, the ultimate goal of optimization is to stabilize system performance. Previous research revealed that system performance is closely related to the following indicators:

The compensated load power factor (PF),

$$PF = \frac{P_L}{V_L I} = \frac{G_{L1}V_{L1}^2 + \sum_{h\geq 2} G_{Lh}V_{Lh}^2}{\sqrt{\left(I_1^2 + \sum_{h\geq 2} I_h^2\right)\left(V_{L1}^2 + \sum_{h\geq 2} V_{Lh}^2\right)}} \tag{19}$$

The compensated load-displacement power factor (DPF),

$$DPF = \frac{P_{L1}}{V_{L1}I_1} = \frac{G_{L1}V_{L1}}{I_1} \tag{20}$$

Transmission loss is calculated as,

$$P_{LOSS} = \sum_h I_h^2 R_h \tag{21}$$

Transmission efficiency is obtained by,

$$\eta = \frac{P_L}{P_L + P_{LOSS}} \tag{22}$$

Compensated $VTHD$ at the load terminals,

$$VTHD = \frac{\sqrt{\sum_{h\geq 2} V_{Lh}^2}}{V_{L1}} \tag{23}$$

Similarly, compensated $ITHD$ for the utility supply current is given below,

$$ITHD = \frac{\sqrt{\sum_{h\geq 2} I_h^2}}{I_1} \tag{24}$$

According to [43], harmonic pollution (HP) can be approximated as follows:

$$HP = \sqrt{VTHD^2 + ITHD^2} \tag{25}$$

The smaller the HP value, the better the filtering effect of the harmonic power filter. Therefore, based on meeting all the variable constraints, this paper searches for the optimal solution to reduce harmonic pollution as much as possible. In the following work, we list the constraint conditions in detail.

On the one hand, the present study selects a certain range of values as below to limit the filter compensation parameters (X_L, X_C, and K):

- $0 \leq X_L \leq 1$
- $0 \leq X_C \leq 10$
- $0 \leq K \leq 20$

On the other hand, the limitation of the harmonic level is also required by the IEEE standard 519-2014 [44]:

- $VTHD \leq VTHD_{lim}$, $VTHD_{lim}$ is set to limit VTHD, which expresses the rated voltage percentage corresponding to the bus voltage level at the PCC.
- $ITHD \leq ITHD_{lim}$, $ITHD_{lim}$ expresses a standard current percent relates to the system short circuit ratio for limiting ITHD value.

Furthermore, there is another parameter $\varepsilon(<10^{-2})$ that cannot be ignored in this research, the parameter stands for the error value between the desired power factor (PF_{goal}) and the actually returned power factor (PF), the definition is indicated as formula (26).

$$PF = PF_{goal} \pm \varepsilon \tag{26}$$

With regards to the optimization objective, we introduce the parameter HP_{APP} in [11] proposed by Biswas *et al.* As mentioned in previous studies, HP_{APP} means the deviation between THD values and their control boundaries as written below:

$$HP_{APP} = |VTHD_{lim} - VTHD| + |ITHD_{lim} - ITHD| \tag{27}$$

$$f(X_L, X_C, L) = -HP_{APP} \tag{28}$$

From formula (27), we can observe that the larger the HP_{APP}, the smaller the values of THD (i.e., VTHD and ITHD) since they are within the corresponding range of positive values and have a tendency to move away from the control boundaries. Moreover, it is clear from formula (28) that when the system meets the constraint conditions, there is an optimization function with '$-HP_{APP}$' (negative) as the single objective, the function variables include the passive inductance (X_L), the capacitance reactance (X_C), and the gain of the active filter (K). Furthermore, the value of HP is calculated by the system compensator parameters (X_L, X_C, and K) determined in the above function, so the harmonic pollution (HP) is related to HP_{APP}.

In this paper, the heuristic search scheme is adopted to achieve the minimum of the optimization function which is to maximize HP_{APP}. As a result, the THD value is reduced effectively, and then the original aim of diminishing the harmonic pollution (HP) in this study is realized.

III. RELATED WORK OF ALGORITHMS

A. META-HEURISTIC ALGORITHMS

Meta-heuristic algorithms fall in the category of stochastic optimization, and they are not dependent on the surface gradient for optimization [45]. All meta-heuristics are constructed based on intuitive or empirically. They combined a random algorithm and a local search algorithm, most of them draw inspiration from nature. Although there are specific differences in the optimization mechanism of various meta-heuristic algorithms, the optimization process is relatively similar [45].

The earliest meta-heuristic algorithm that has become a research hotspot may be the genetic algorithm (GA) proposed

by Holland in 1975 [46]. GA is a global parallel search algorithm inspired by the biological evolution and genetic methods of survival of the fittest. Another typical meta-heuristic algorithm PSO with global optimization performance was proposed by Kennedy and Eberhart in 1995 [34]. It is a global random optimization algorithm based on swarm intelligence, which imitates the foraging behavior of birds. In 1997 [47], Storn *et al.* proposed a stochastic search algorithm differential evolution algorithm (DE) for real variable function optimization, which is a further expansion of genetic algorithms, using selection, crossover, and mutation to update population individuals. Similar to PSO, the artificial bee colony algorithm (ABC) is also a swarm intelligence algorithm proposed by simulating the behavior of biomes which simulates the behavior of bees. It was first proposed by Karaboga in 2005 [48], and it is also one of the most popular meta-heuristic algorithms. In 2011 [35], Rao *et al.* proposed the TLBO which simulates the traditional classroom teaching process, and it does not require any algorithm-specific parameters. The optimization process of the algorithm is divided into the teacher phase and the learner phase. Another popular meta-heuristic algorithm moth-flame optimization algorithm (MFO) was proposed by Mirjalili in 2015 [33], the MFO algorithm is also a new swarm intelligence bionic algorithm which has been successfully applied for many problems.

In recent years, more and more new meta-heuristic algorithms have been proposed and widely used in engineering and artificial intelligence. Most recently proposed new algorithms are improved algorithms for specific problems, such as L-SHADE [11], MLBSA [17], CSSA [32], etc. Nevertheless, there are still many algorithms inspired by nature, such as multi-verse optimizer (MVO) [36], grasshopper optimisation algorithm (GOA) [49], and so on.

B. SALP SWARM ALGORITHM (SSA)

The salp swarm algorithm proposed by Mirjalili is a group algorithm based on salps behavior [18]. Salps belonging to the Salpidae family, its body construction is transparent and bucket. Besides, the swarming behavior of salps looks like a chain, so the salp swarm is called the salp chain.

The salp chain can be divided into a leader and followers, corresponding to two different stages called LP and FP, respectively. The basic introduction to these two phases is as follows.

1) LEAD PHASE (LP)

The inspiration of the algorithm was the salps' behavior and the synergy effect for searching the food target in the abyssal sea. The target of the salps population is the food source inside the deep water. In the LP, the salp of the leader group only moves based on the food source, then the position of leader is updated as follows:

$$X_{\mathrm{j}}^{1} = \begin{cases} F_{\mathrm{j}} + \mathrm{c} \times \left[\left(ub_{\mathrm{j}} - lb_{\mathrm{j}} \right) \times r_1 + lb_{\mathrm{j}} \right] & r_2 \le 0 \\ F_{\mathrm{j}} - \mathrm{c} \times \left[\left(ub_{\mathrm{j}} - lb_{\mathrm{j}} \right) \times r_1 + lb_{\mathrm{j}} \right] & r_2 > 0 \end{cases} \tag{29}$$

where X_{j}^{i} represents the position of the ith salp in the jth dimension, there is only a leader in this algorithm, so X_{j}^{1} shows the leader slap's position in the jth dimension. F_{j} indicates the food target position in the jth dimension; ub_{j} is the upper bound in the jth dimension when lb_{j} is the lower bound in the jth dimension. The factor c which can be counted as Eq. (30) is set to balance exploration and exploitation; r_1 and r_2 are two random numbers between 0 and 1.

$$c = 2e^{-\left(\frac{4l}{L}\right)^2} \tag{30}$$

where l shows the current iteration and L shows the maximum iteration. These parameters and equations determine the position of the updated leader in the jth dimension. The mentioned above position update process is the lead phase (LP).

2) FOLLOW PHASE (FP)

After updating the position of the leader, the SSA began to update the followers' position during the FP. In the FP, the salps of the follower group update their positions according to the positions of other salps. Here we can calculate the next position for each follower by using Eq. (31):

$$X_{\mathrm{j}}^{i} = X_{\mathrm{j}}^{i} + \frac{1}{2}\left(X_{\mathrm{j}}^{i-1} - X_{\mathrm{j}}^{i} \right) \tag{31}$$

As described in the LP, X_{j}^{i} means the ith salp in the jth dimension, X_{j}^{i-1} represents the previous salp in the jth dimension. This equation is derived from Newton's laws of motion, and through Eq. (31) the follower group can be regenerated. The above process is the original FP.

C. SPIRAL FLIGHT SEARCH (SFS) STRATEGY

The spiral flight search strategy was formulated in the MFO algorithm proposed in 2015 [33]. The MFO algorithm is a new swarm intelligence bionic algorithm, and the whole population is composed of a swarm of moths. The spiral flight search strategy acts as a navigation behavior in the group, which simulates the process of moths circling towards the flame.

In MFO, each moth flies to its matching flame through a spiral shape. The helix line should meet the conditions that start from moth and end to the flame. Also, the floating range cannot exceed the search space. Based on these three conditions, the mathematical simulation of the spiral flight behavior in the MFO algorithm can be concluded as the SFS strategy, which can be mathematically described as:

$$X_{\mathrm{j}}^{i} = F_{\mathrm{j}}^{i} + e^{bt} \cdot \cos 2\pi t \cdot \left| F_{\mathrm{j}}^{i} - X_{\mathrm{j}}^{i} \right| \tag{32}$$

where X_{j}^{i} means the ith moth in the jth dimension which is similar to the expression in the salp algorithm; F_{j}^{i} means the corresponding flame of the ith moth in the jth dimension, and b is a constant coefficient defining the flight search's helix shape; t is a uniformly distributed random number among $[-1, 1]$. In the case of different t values, different moths fly helically towards the matching flame in one dimension are illustrated in Fig. 6.

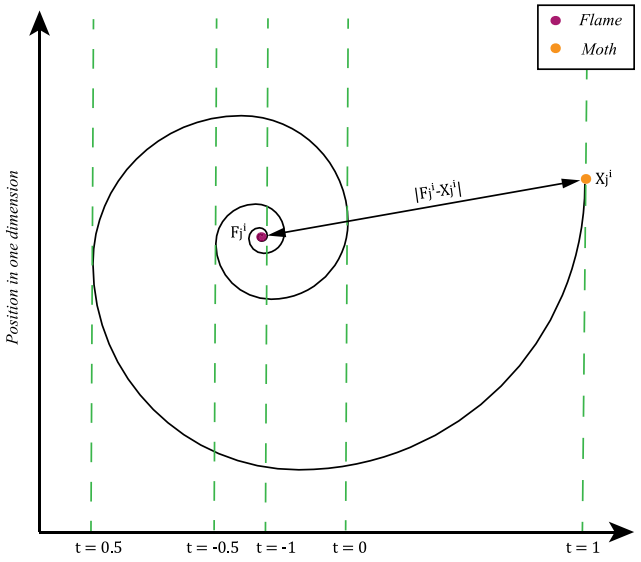

FIGURE 6. SFS strategy of moths, the helix of flight search.

IV. THE PROPOSED ALGORITHM

As mentioned above, the original SSA divides the salp swarm into two groups for seeking the optimal solution, and the two groups correspond to two different phases, respectively. In the LP, the leader salp approaches the food source according to the upper and lower limit of variables. Although the LP attempts to optimize by moving towards the food source, the randomness of random numbers (r_1, r_2) may have a significant impact on the optimization effect. Furthermore, during the FP, the follower salp only selects the previous one salp to switch information. As a result, the exchanged information may be limited, which may limit the exploitation capability of the followers, and lead to poor local searching ability. To optimize the performance of SSA, we propose the ISSA-SFS algorithm.

For making a better tradeoff between exploration and exploitation of the newly proposed algorithm, the two phases are improved to exploit and explore the salp population, respectively. So, the leader group should improve its global search capability, while the follower group should enhance the diversity and local search capability of the population.

A. IMPROVED LEAD PHASE (ILP)

During the LP of the original SSA, the leader salp is the individual with the currently best fitness value. Note that only one single leader in the leader group is led by the food source and limited by boundary conditions. Moreover, due to the structure of the search space is similar to chain structure, the updating degree of salp search positions in the LP is still low, and the uncertainty is large. After the analysis, the original SSA can be optimized by improving its search space.

The ISSA-SFS adopts a multiple leader (ML) strategy that multiple leaders are selected to lead the salp swarm approaching the food target, and then this strategy evolves the single-chain structure to a multi-chain structure. Therefore, the algorithm reduces the uncertainty of the search process and avoids the population being stuck in local optimization due to a single search space direction. At the same time, we introduce the spiral flight search (SFS) strategy in the MFO algorithm to find new promising areas and make the population find a better position more efficiently.

Note that the number of leaders in the leader group is denoted as $N1$. The value of $N1$ can be adjusted as a parameter that is always greater than one.

The improved lead phase (ILP) is given as:

$$X_j^i = F_j^i + 4e^{2bt} \cdot \cos \pi t \cdot \left| F_j^i - X_j^i \right| \tag{33}$$

where X_j^i represents the ith salp's position in the jth dimension. F_j indicates the food target position in the jth dimension. The constant b is the coefficient defining the flight search's helix shape, the parameter is set to balance exploration and exploitation; t is a random number in the range $[-1, 1]$ can be counted as Eq. (35), it is related to an adaptive parameter 'a' which can be formulated by Eq.(34) as follows:

$$\mathrm{a} = -1 - \frac{\mathrm{nfes}}{\max\_\mathrm{nfes}} \tag{34}$$

$$t = rand \cdot (a - 1) + 1 \tag{35}$$

B. IMPROVED FOLLOW PHASE (IFP)

As mentioned above, selecting only the previous one salp in FP for information exchange may lead to poor local search capabilities and limited capabilities to follow. In order to overcome these shortcomings, we develop a random learning (RL) strategy for the following new phase IFP.

In the FP of the original SSA, the new position of each salp is only related to the previous one salp's position, the position of each follower is updated according to its distance from the last individual. By this inspiration, in order to enhance the diversity of the population, we spread different samples across the solution space. The new algorithm ISSA-SFS employs two other salps to update the salp's position as samples, and then each follower moves according to the distance between the two salps. The above operation is the proposed RL strategy which enables the improved follow phase (IFP) to prevent salps from repeatedly searching the same solution area, and the exploitation ability of follower group individuals with poor fitness value is enhanced.

The IFP is formulated as:

$$X_j^i = X_j^i + \frac{1}{2}\left(X_j^{s_1} - X_j^{s_2}\right) \tag{36}$$

where s_1, s_2 are random integers in $\{1, NP$, and they are all different from i, and they are different from each other.

C. PROCEDURE OF ISSA-SFS

The execution procedure of ISSA-SFS is described by the pseudo-code in Algorithm 1 and the flow chart in Fig. 7 as follows. Here, the parameter "$N1$" is set to the integer closest to the value of $NP/3$, which means the leader group is approximately the first third of the entire salp swarm.

Algorithm 1 ISSA-SFS Algorithm

INPUT: Control parameters: NP, max_nfes
OUTPUT: The optimal solution F, the best fitness value f [F]

/***Initialization***/
Set nfes = 0;
Randomly initialize each salp X_i, $i \in \{1, 2, \ldots, NP\}$ considering ub and lb;
Evaluate the fitness value f $[X_i]$ of each salp, $i \in \{1, 2, \ldots, NP\}$
nfes = nfes + NP;
Ranking the whole NP individuals salps' fitness values;
F = the best search agent;
/***Main Loop***/
while (end condition is not satisfied) do
l = l + 1;
update parameters a and t
    for each individual (X_i)
        //improved lead phase
        if ($i >= 1$ && $i < N1 + 1$)
    update the position of the leader group individuals by Eq. (33)
        //improved follow phase
        else if ($i > N1$ && $i < NP + 1$)
    Update the position of the follower group individuals by Eq. (36)
        end if
    end for
Modify the salps according to ub and lb
nfes = nfes + NP
Compare the fitness values of the salps and return the best salp F
end while

D. TIME COMPLEXITY ANALYSIS OF ISSA-SFS

The computational complexity of the original SSA mainly relies on two parts, namely the position updating process $O(PUP)$ and the position evaluating process $O(PEP)$. Suppose that D, N, and L are the number of dimensions, the solution number, and the maximum number of iterations, respectively. Therefore, $O(PUP)$ and $O(PEP)$ are assessed as $O(L*N*D)$ and $O(L*N*Cof)$, where Cof indicates the cost of the objective function. The total computational complexity of the SSA algorithm can be formulated as:

$$O(SSA) = O(L * (N * D + N * Cof)) \quad (37)$$

In order to enhance the searching ability of the population, we used the Quicksort algorithm in ISSA-SFS to sort the salp swarm according to the fitness value. In ISSA-SFS, its computational complexity mainly depends on three parts: position updating process $O(PUP)$, position evaluating process $O(PEP)$, and sorting mechanism of salps $O(SORT)$. Similarly, $O(PUP)$ and $O(PEP)$ are also assessed as $O(L * N * D)$ and $O(L * N * Cof)$. Particularly, the sorting algorithm is executed in each iteration, and $O(SORT)$ is between $O(NlogN)$ and $O(N^2)$ corresponding to the best and worst case, respectively. Therefore, in the worst case, the overall computational complexity of ISSA-SFS can be assessed as:

$$O(ISSA - SFS) = O(L * (N * D + N * Cof + N^2)) \quad (38)$$

From the above analysis, the computational cost of the proposed ISSA-SFS is slightly more than the SSA algorithm, which is a reasonable price to pay for better performance.

V. EXPERIMENTAL RESULT AND DISCUSSION

A. TEST CASES AND DATASET

For the two HAPF configurations mentioned in section 2 of this article, four case studies are conducted using ISSA-SFS, respectively. The specific dataset is listed as Table 1 below, where the supply bus voltage is 4.16kV, and the total three-phase apparent load is (5100 + j4965) kV. Furthermore, the system's short-circuit capacity is 80MVA. The first three cases mentioned above are from the actual plant within an example of IEEE [50], and the last one is the same as [11]. The source and load harmonics of these cases are higher than in many other cases, so it is difficult to obtain appropriate optimized parameters relatively, which implies considerable research significance.

TABLE 1. Cases studies of an industrial plant under study [11].

Parameters	Case 1	Case 2	Case 3	Case 4
Short Circuit (MVA)	80	80	80	80
R1 (Ω)	0.02163	0.02163	0.02163	0.02163
X1 (Ω)	0.2163	0.2163	0.2163	0.2163
RL1 (Ω)	1.7421	1.7421	1.7421	1.7421
XL1 (Ω)	1.696	1.696	1.696	1.696
V1 (kV)	2.40	2.40	2.40	2.40
V5 (%V1)	0.00	2.00	4.00	4.00
V7 (%V1)	0.00	1.50	3.00	3.00
V11 (%V1)	0.00	1.00	2.00	3.00
V13 (%V1)	0.00	0.50	1.00	1.20
IL5 (%IL)	40.00	40.00	40.00	40.00
IL7 (%IL)	6.00	6.00	6.00	6.00
IL11 (%IL)	2.00	2.00	2.00	2.00
IL13 (%IL)	1.00	1.00	1.00	1.00

In this work, we assume that the source harmonics and load harmonics are time-invariant. Additionally, the source resistances R_h and load resistances R_{Lh} denote unrelated to frequency, their values are illustrated in Table 1 which corresponds to R_1 and R_{L1} respectively. In the uncompensated system, the displacement power factor of 71.65% is linked to the total apparent load value, and it can be enhanced to 95% by adding 3289 kvar reactive power. The power factor value of 95% is selected as PF_{gaol} in this study. Moreover, the total harmonic distortion factor is limited under 5% in this low-voltage system under study, so both the value of $VTHD_{lim}$ and $ITHD_{lim}$ are considered to be 5% for lower THD. Note that meeting these constraints are essential for evaluating the objective function, as a numerical optimization technique, the evaluation process included an exact penalty

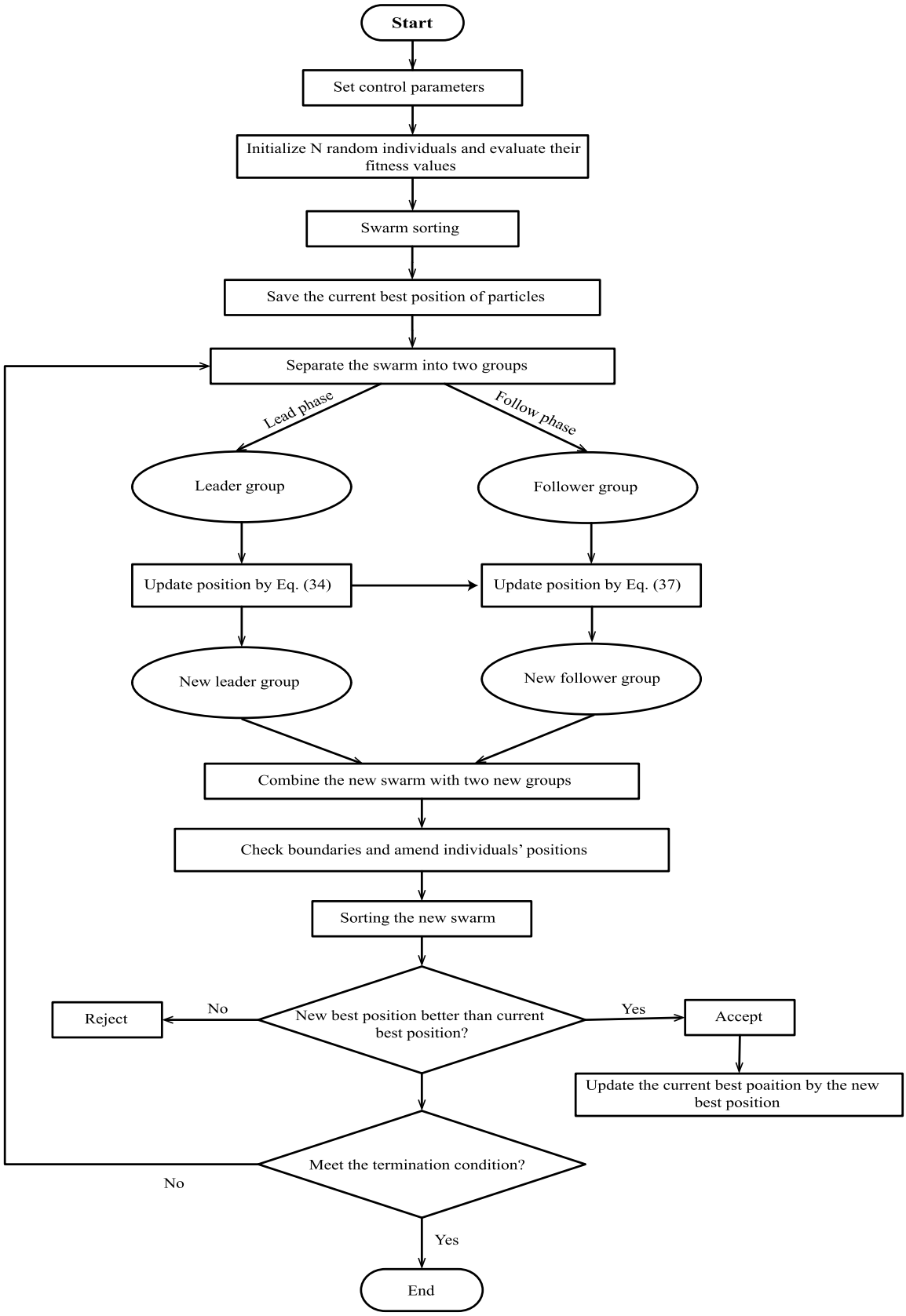

FIGURE 7. Flow Chart of ISSA-SFS.

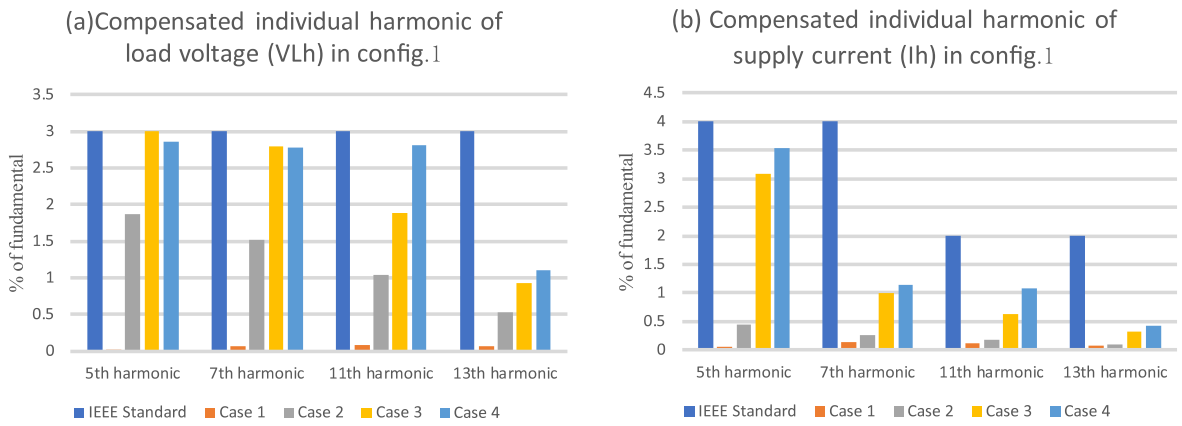

FIGURE 8. Harmonic content for all cases with compensated config.1 'APF in series with shunt passive filter.'

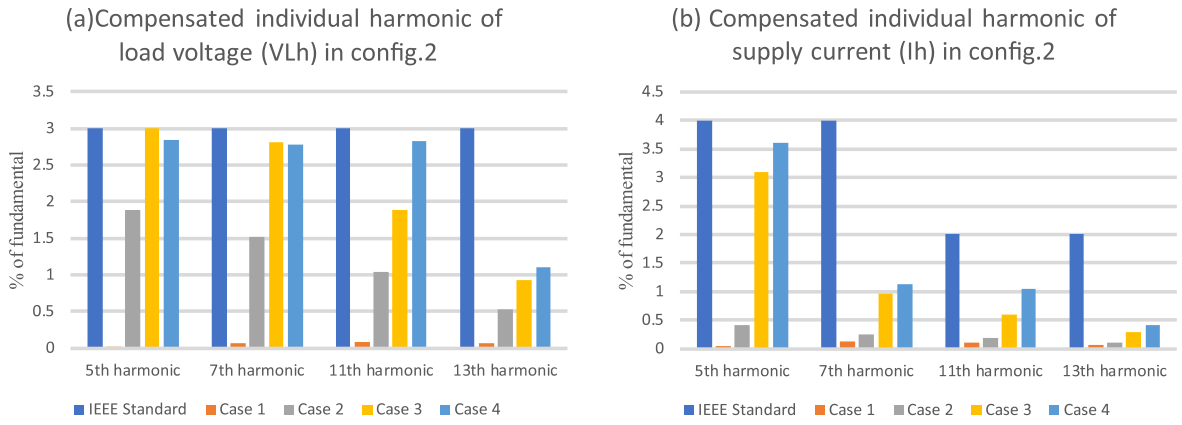

FIGURE 9. Harmonic content for all cases with compensated config.2 'combined series APF and shunt passive filter.'

function which is used for penalizing the violations of constraints by discarding the abnormal solutions. For this reason, we propose a concept of pass rate, which is counted based on the rate of obtaining feasible solutions that satisfy the boundaries. The pass rate is an assessment indicator that can be utilized for analyzing the stability of optimization techniques.

B. COMPENSATING EFFECT OF HAPF CONFIGURATIONS

HAPF optimization aims to suppress the harmonics in the power system by determining the compensator parameters. Therefore, the better the parameters of the compensator, the better the effect of harmonic suppression. In general, the determination of the control gain is complicated, but it has a more obvious impact on the effect because the gain K of the active filter has an inverse relationship with the voltage harmonics on the system bus. When the gain increases, the reduction of voltage harmonics will lead to a better compensation effect directly [42]. According to the test results, although the circuits and filtering principles of the discussed HAPF topologies are different, the system parameters of the two HAPF topologies are almost similar when studying the medium voltage system.

For the discussed config.1 'APF in series with shunt passive filter' and config.2' combined series APF and shunt passive filter', the optimized total harmonic distortion is decreased obviously as Figures 8 and 9 show, respectively. The individual harmonics of case 3 and case 4 are significantly higher than the first two cases, which means challenges to some extent. Nevertheless, the illustrated technique has still provided possible results that the compensated individual harmonics of load voltage and supply current are within the IEEE standard [44].

C. RESULTS OF THE COMPARED ALGORITHMS

1) PARAMETER SETTINGS

In ISSA-SFS, the number of leaders is adjustable, and the value of $N1$ plays an important role in balancing the exploration and exploitation of ISSA-SFS. Thus, it is necessary to determine a suitable $N1$ value for obtaining more satisfactory results. For intuitive comparison, we evaluate the ISSA-SFS with three different $N1$ values shown in Table 2. It can be observed that ISSA-SFS is slightly sensitive to the value of $N1$. Although the results under different conditions are different, the performances of ISSA-SFS with different parameters are comparable. In terms of the HAPF

TABLE 2. Statistical results of ISSA-SFS with different settings of $N1$ values.

HAPF Structure	Case no.	Parameter setting*	Harmonic Pollution (in %)			
			Best	Worst	Mean	SD
config.1	Case 1	$N1=[NP/2]$	**0.236**	0.493	0.244	4.54E-02
		$N1=[NP/3]$	**0.236**	**0.237**	**0.236**	**4.35E-04**
		$N1=[NP/4]$	**0.236**	0.239	**0.236**	8.31E-04
	Case 2	$N1=[NP/2]$	2.738	2.777	2.750	**7.18E-03**
		$N1=[NP/3]$	2.726	**2.759**	2.747	7.24E-03
		$N1=[NP/4]$	**2.725**	2.760	**2.746**	8.48E-03
	Case 3	$N1=[NP/2]$	**5.672**	**5.888**	5.783	1.08E-01
		$N1=[NP/3]$	**5.672**	**5.888**	**5.749**	**1.03E-01**
		$N1=[NP/4]$	**5.672**	**5.888**	5.770	1.07E-01
	Case 4	$N1=[NP/2]$	**6.340**	6.445	6.343	1.86E-02
		$N1=[NP/3]$	**6.340**	**6.340**	**6.340**	**4.58E-14**
		$N1=[NP/4]$	**6.340**	**6.340**	**6.340**	1.76E-12
config.2	Case 1	$N1=[NP/2]$	**0.227**	0.459	0.235	4.08E-02
		$N1=[NP/3]$	**0.227**	**0.230**	**0.228**	6.72E-04
		$N1=[NP/4]$	**0.227**	**0.230**	**0.228**	**5.61E-04**
	Case 2	$N1=[NP/2]$	2.740	**2.761**	2.752	**5.46E-03**
		$N1=[NP/3]$	2.738	2.762	2.750	5.86E-03
		$N1=[NP/4]$	**2.713**	2.771	**2.748**	1.23E-02
	Case 3	$N1=[NP/2]$	**5.681**	**5.906**	**5.768**	**1.10E-01**
		$N1=[NP/3]$	**5.681**	**5.906**	5.783	1.12E-01
		$N1=[NP/4]$	**5.681**	**5.906**	5.797	1.13E-01
	Case 4	$N1=[NP/2]$	**6.370**	6.506	6.380	3.25E-02
		$N1=[NP/3]$	**6.370**	**6.426**	6.373	9.87E-03
		$N1=[NP/4]$	**6.370**	**6.370**	**6.370**	**2.31E-10**

* The operator "[]" means rounding to the nearest whole number.

TABLE 3. Control parameter setting of different algorithms.

Algorithm	Control parameters
SSA [18]	$NP=100$
MFO [33]	$NP=100; b=1$
MVO [36]	$NP=100; WEP_{max}=1; WEP_{min}=0.2; p=6$
PSO [34]	$NP=100; W_{start}=0.9; W_{end}=0.4; c1=2; c2=2;$ $V_{max}=0.5; V_{min}=-0.5$
TLBO [35]	$NP=100$
L-SHADE [11]	$NP=100; NP_{min}=4; \mu F_r^{(0)}=\mu CR_r^{(0)}=0.5$
ISSA-SFS	$NP=100; b=1; N1=33$

parameter extraction problem studied in this paper, we set $N1=[NP/3]$.

In Section 5.1 and 5.2, the filtering effect of ISSA-SFS is verified. To verify the competitiveness, we compared the experimental statistical results of ISSA-SFS and various other well-established algorithms. Including the original SSA [18], MFO [33], MVO [36], PSO [34], TLBO [35], and a recent proposed high-performance method (L-SHADE) [11]. Note that MFO and MVO have been proved to be competitive in solving real problems with unknown search spaces [48]. Both PSO and TLBO are classic and popular algorithms widely used in diverse fields. As for L-SHADE, it is a recently developed competitive algorithm that performs well in HAPF parameter estimation. Specifically, Table 3 shows the parameter settings of the above algorithm. These parameters are selected through multiple tests to obtain relatively good parameters, and some of these basic algorithms have more than one form of search space. For example, concerning the PSO algorithm, the test is adopted with the linear decreasing inertia weight (LDIW), which is recognized to be the best dynamic strategy.

For the above algorithms, the maximum number of function evaluations is equally set to 50000 in each run. Simultaneously, the obtained data can guarantee the consistency of the output results when we run 31 times for each algorithm. Furthermore, all the comparative algorithms are implemented in Matlab R2018b and then executed on a PC with an Intel Core i5-8265U CPU @ 3.40 GHz with 8GB RAM, under the Windows 10 64-bit OS. Thus, the comparison between the optimization algorithms is fair.

2) STATISTICAL ANALYSIS

In this part, the mentioned harmonic pollution (HP) in equation (25) is reported in Tables 4 and 5 as follows. Table 4 shows the statistical results of the HAPF config.1, including the best, worst, mean, standard deviation of HP values, and the total CPU time for the seven algorithms shown in Table 4. Likewise, these values of HAPF config.2 are reported in Table 5. As is well known, the best value means the accuracy, and the mean value means the reliability of the technique, so the following data can reflect the algorithms' performance straight. For the sake of intuitive comparison, the minimum of best, worst, mean, standard deviation, the least running time, and the maximum passing rate are all highlighted in **boldface**.

As can be seen from Table 4, in terms of the best value, the ISSA-SFS can reach the optimum solution when the algorithm is used to optimize the HAPF configuration 1. Further analysis finds that the best value of almost all algorithms except the original SSA in case 1 can obtain the minimum (0.236), and only SSA and TLBO cannot reach the best value in cases 3 and 4. Nevertheless, a significantly optimal value (2.726) is achieved only by ISSA-SFS in case 2, which shows the excellent accuracy of ISSA-SFS. For the worst value, L-SHADE takes the minimum of worst values in case 2, and ISSA-SFS provides the second-best results simultaneously. Furthermore, ISSA-SFS provides the optimum HP values under other study cases which is significantly lower than other algorithms. As for the mean level of HP, ISSA-SFS outperforms other algorithms obviously in all cases. The standard deviations of ISSA-SFS are also smaller than other algorithms in cases 1 and 4.

For the HAPF configuration 2, the best, worst, mean, and standard deviation results are not significantly changed, the performance of each algorithm can also be indicated in Table 5. Based on these statistical results, obviously that ISSA-SFS causes significant control upon HP percent, the accuracy, and robustness of ISSA-SFS are better than other algorithms. MFO and L-SHADE are also highly competitive for attaining the best values. However, their mean level and worst level are not good indeed. As for MVO and TLBO, their results are unstable, but the overall performance of TLBO is better than MVO due to the apparent difference between their passing rates. Another comparable algorithm, PSO, can provide the optimal values as data shows, but its passing rate is the lowest among these discussed

TABLE 4. Statistical results for different algorithms with HAPF config.1.

Case no.	Algorithm	Harmonic Pollution (in %)				CPU time (s)	Passing rate (%)	Wilcoxon signed-rank test
		Best	Worst	Mean	SD			
Case 1	SSA	0.243	0.987	0.492	1.73E-01	**90.71**	**100.00**	+1
	MFO	**0.236**	0.493	0.402	1.23E-01	96.38	**100.00**	0
	PSO	**0.236**	0.501	0.404	1.23E-01	116.98	**100.00**	+1
	MVO	**0.236**	0.496	0.387	1.25E-01	95.56	**100.00**	+1
	TLBO	**0.236**	0.461	0.285	7.93E-02	104.17	**100.00**	0
	L-SHADE	**0.236**	0.493	0.252	6.32E-02	110.00	**100.00**	-1
	ISSA-SFS	**0.236**	**0.237**	**0.236**	**4.35E-04**	104.35	**100.00**	
Case 2	SSA	2.744	3.095	2.912	1.12E-01	**90.24**	**100.00**	+1
	MFO	2.750	2.954	2.869	9.87E-02	96.70	**100.00**	+1
	PSO	2.734	2.970	2.858	1.01E-01	115.27	67.74	+1
	MVO	2.733	2.962	2.868	9.80E-02	96.07	**100.00**	+1
	TLBO	2.742	2.952	2.837	9.49E-02	104.89	**100.00**	+1
	L-SHADE	2.752	**2.752**	2.752	**2.23E-09**	113.74	**100.00**	+1
	ISSA-SFS	**2.726**	2.759	**2.747**	7.24E-03	106.42	**100.00**	
Case 3	SSA	5.755	6.189	5.954	1.05E-01	**90.66**	70.97	+1
	MFO	**5.672**	5.907	5.847	8.59E-02	97.38	**100.00**	0
	PSO	**5.672**	**5.888**	5.878	**4.50E-02**	114.32	70.97	+1
	MVO	**5.672**	5.891	5.868	6.40E-02	97.06	**100.00**	+1
	TLBO	5.675	**5.888**	5.863	5.97E-02	103.23	**100.00**	+1
	L-SHADE	**5.672**	**5.888**	5.804	1.02E-01	109.57	93.55	0
	ISSA-SFS	**5.672**	**5.888**	**5.749**	1.03E-01	105.76	**100.00**	
Case 4	SSA	6.349	7.002	6.630	3.03E-01	**90.55**	16.13	+1
	MFO	**6.340**	6.978	6.445	2.34E-01	96.47	**100.00**	0
	PSO	**6.340**	6.978	6.468	2.55E-01	116.03	83.87	+1
	MVO	**6.340**	6.979	6.432	2.23E-01	95.75	45.16	+1
	TLBO	6.343	7.069	6.484	1.71E-01	101.25	80.65	+1
	L-SHADE	**6.340**	6.433	6.360	2.72E-02	113.83	64.52	+1
	ISSA-SFS	**6.340**	**6.340**	**6.340**	**4.58E-14**	106.28	**100.00**	

TABLE 5. Statistical results for different algorithms with HAPF config.2.

Case no.	Algorithm	Harmonic Pollution (in %)				CPU time (s)	Passing rate (%)	Wilcoxon signed-rank test
		Best	Worst	Mean	SD			
Case 1	SSA	0.240	0.820	0.456	1.45E-01	**92.06**	**100.00**	+1
	MFO	**0.227**	0.459	0.392	1.05E-01	104.80	**100.00**	+1
	PSO	0.228	0.465	0.416	9.12E-02	116.16	83.87	+1
	MVO	**0.227**	0.461	0.364	1.12E-01	96.13	**100.00**	+1
	TLBO	**0.227**	0.459	0.305	9.31E-02	102.96	**100.00**	+1
	L-SHADE	**0.227**	0.459	0.235	4.09E-02	113.44	**100.00**	0
	ISSA-SFS	**0.227**	**0.230**	**0.228**	**6.72E-04**	106.88	**100.00**	
Case 2	SSA	2.755	3.074	2.926	8.95E-02	**90.97**	**100.00**	+1
	MFO	2.750	2.950	2.880	9.31E-02	104.32	**100.00**	+1
	PSO	2.759	2.972	2.888	8.47E-02	116.22	87.10	+1
	MVO	2.741	2.959	2.833	9.52E-02	95.13	**100.00**	+1
	TLBO	**2.712**	2.949	2.829	9.23E-02	102.54	**100.00**	+1
	L-SHADE	2.754	2.949	2.773	5.76E-02	111.62	**100.00**	+1
	ISSA-SFS	2.738	**2.762**	**2.750**	**5.86E-03**	105.26	**100.00**	
Case 3	SSA	5.718	6.135	5.959	9.16E-02	**90.39**	74.19	+1
	MFO	**5.681**	5.975	5.872	8.47E-02	97.03	**100.00**	+1
	PSO	**5.681**	**5.906**	5.850	9.76E-02	115.46	51.61	+1
	MVO	**5.681**	5.909	5.856	9.42E-02	96.79	**100.00**	+1
	TLBO	5.684	**5.906**	5.880	**5.33E-02**	101.31	**100.00**	+1
	L-SHADE	**5.681**	**5.906**	5.831	1.06E-01	112.42	96.77	+1
	ISSA-SFS	**5.681**	**5.906**	**5.761**	1.08E-01	106.55	**100.00**	
Case 4	SSA	6.445	6.639	6.542	9.71E-02	**91.04**	6.45	+1
	MFO	**6.370**	7.057	6.393	1.23E-01	96.94	96.77	0
	PSO	**6.370**	7.057	6.599	3.24E-01	114.09	9.68	+1
	MVO	6.372	7.057	6.601	3.23E-01	95.56	19.35	+1
	TLBO	6.416	6.844	6.609	1.37E-01	104.02	58.06	+1
	L-SHADE	**6.370**	6.606	6.397	5.10E-02	109.60	90.32	+1
	ISSA-SFS	**6.370**	**6.426**	**6.373**	**9.87E-03**	104.57	**100.00**	

algorithms, which means that the algorithm is difficult to meet the constraints, so PSO is unsuitable for this specific problem.

With respect to the total CPU time, SSA takes significantly less operational time than other comparative algorithms in all cases. According to the results, ISSA-SFS cannot spend the

TABLE 6. Compensated parameters of best results obtained by ISSA-SFS.

HAPF Structure	Case no.	Optimized parameters					
		$X_L(\Omega)$	X_C (Ω)	K (Ω)	VTHD (%)	ITHD (%)	HP (%)
config.1	Case 1	0.1040	2.7098	20.00	0.125	0.200	0.236
	Case 2	0.0830	2.6909	20.00	2.668	0.558	2.726
	Case 3	0	2.6159	9.75	4.609	3.306	5.672
	Case 4	0	2.6187	8.47	5.000	3.898	6.340
config.2	Case 1	0.1045	2.7102	20.00	0.121	0.193	0.227
	Case 2	0.0882	2.6962	20.00	2.687	0.525	2.738
	Case 3	0	2.6160	10.31	4.615	3.312	5.681
	Case 4	0	2.6188	8.84	5.000	3.946	6.370

TABLE 7. Effects of different strategies in ISSA-SFS for all cases.

Algorithm	Update process	Criteria	HAPF config.1				HAPF config.2			
			Case 1	Case 2	Case 3	Case 4	Case 1	Case 2	Case 3	Case 4
ISSA-SFS-1	ML strategy RL strategy	Best	**0.236**	2.713	**5.672**	**6.340**	0.227	2.749	5.681	**6.370**
		Worst	0.386	2.950	5.895	6.978	0.459	2.949	5.939	6.544
		Mean	0.269	2.761	5.806	6.361	0.250	2.772	5.803	6.382
		SD	4.23E-02	3.59E-02	1.05E-01	1.13E-01	5.18E-02	4.79E-02	1.12E-01	3.39E-02
		Rank	3	4	4	3	3	4	2	2
ISSA-SFS-2	SFS strategy RL strategy	Best	**0.236**	**2.671**	5.680	6.341	**0.226**	**2.675**	**5.678**	6.378
		Worst	0.641	2.976	5.960	6.653	0.483	2.873	5.972	6.866
		Mean	0.322	2.749	5.784	6.433	0.304	**2.734**	5.817	6.525
		SD	9.32E-02	7.68E-02	**8.46E-02**	7.83E-02	8.17E-02	5.73E-02	**9.88E-02**	1.22E-01
		Rank	4	2	3	4	4	1	3	4
ISSA-SFS-3	SFS strategy ML strategy	Best	**0.236**	2.738	**5.672**	**6.340**	0.227	2.743	5.681	**6.370**
		Worst	0.238	2.762	5.902	6.359	0.459	2.769	5.982	6.449
		Mean	**0.236**	2.750	5.756	6.341	0.235	2.754	5.837	6.384
		SD	5.24E-04	**5.68E-03**	1.06E-01	4.33E-03	4.09E-02	**5.31E-03**	1.04E-01	2.78E-02
		Rank	2	3	2	2	2	3	4	3
ISSA-SFS	SFS strategy ML strategy RL strategy	Best	**0.236**	2.726	**5.672**	**6.340**	0.227	2.738	5.681	**6.370**
		Worst	**0.237**	**2.759**	**5.888**	**6.340**	**0.230**	**2.762**	**5.906**	**6.426**
		Mean	**0.236**	**2.747**	**5.749**	**6.340**	**0.228**	2.750	**5.783**	**6.373**
		SD	**4.35E-04**	7.24E-03	1.03E-01	**4.58E-14**	**6.72E-04**	5.86E-03	1.12E-01	**9.87E-03**
		Rank	**1**	**1**	**1**	**1**	**1**	**2**	1	**1**

least amount of running time, because we employed a sorting mechanism to improve performance. Despite this, ISSS-SFS can still provide better results in the case of relatively little time-consuming.

To fully assess the performance of ISSA-SFS, the Wilcoxon signed-rank test [51] with a significance level of 0.05 between ISSA-SFS and each of the other algorithms are illustrated in Tables 4 and 5, which is a famous nonparametric statistical hypothesis test. Symbol "+1" and "−1" denotes that ISSA-SFS has obviously better and worse performance in the same case, symbol "0" means that there is no significant difference between ISSA-SFS and the compared algorithm. For example, the comparative results between ISSA-SFS and L-SHADE include five symbols "1", two symbols "0", and one symbol "−1" in the eight cases. Five symbols "1" indicate that ISSA-SFS provides 5 considerably superior solutions out of the 8 cases compared with L-SHADE; two symbols "0" mean that ISSA-SFS supplies two statistical equivalent results to L-SHADE on 2 out of the 8 cases; one symbol "−1" indicates that ISSA-SFS has significantly worse solutions than L-SHADE on one out of the 8 cases.

From the test results, it can be observed that ISSA-SFS supplies considerably better results than all competitors in most cases discussed. The results further confirm that ISSA-SFS achieves the best overall performance among the compared algorithms.

Based on the above data obtained in the experiment, we can list the harmonic distortion values, and the compensated parameters corresponded to the lowest harmonic pollution illustrated in Table 6. By using these HAPF compensated parameters, we can achieve the goal of suppressing harmonic pollution in the design of the HAPF filter procedure, thereby reducing the power system loss and improving the quality of power owned by the user.

D. EFFECTS OF DIFFERENT STRATEGIES IN ISSA-SFS

To verify the impact of the three new strategies in ILP and IFP on ISSA-SFS, we conducted some experiments based on ISSA-SFS and three ISSA-SFS variants (denoted as ISSA-SFS-1, ISSA-SFS-2, and ISSA-SFS-3, respectively). The proposed algorithm ISSA-SFS integrates three different strategies: the spiral flight search (SFS) strategy, the multiple

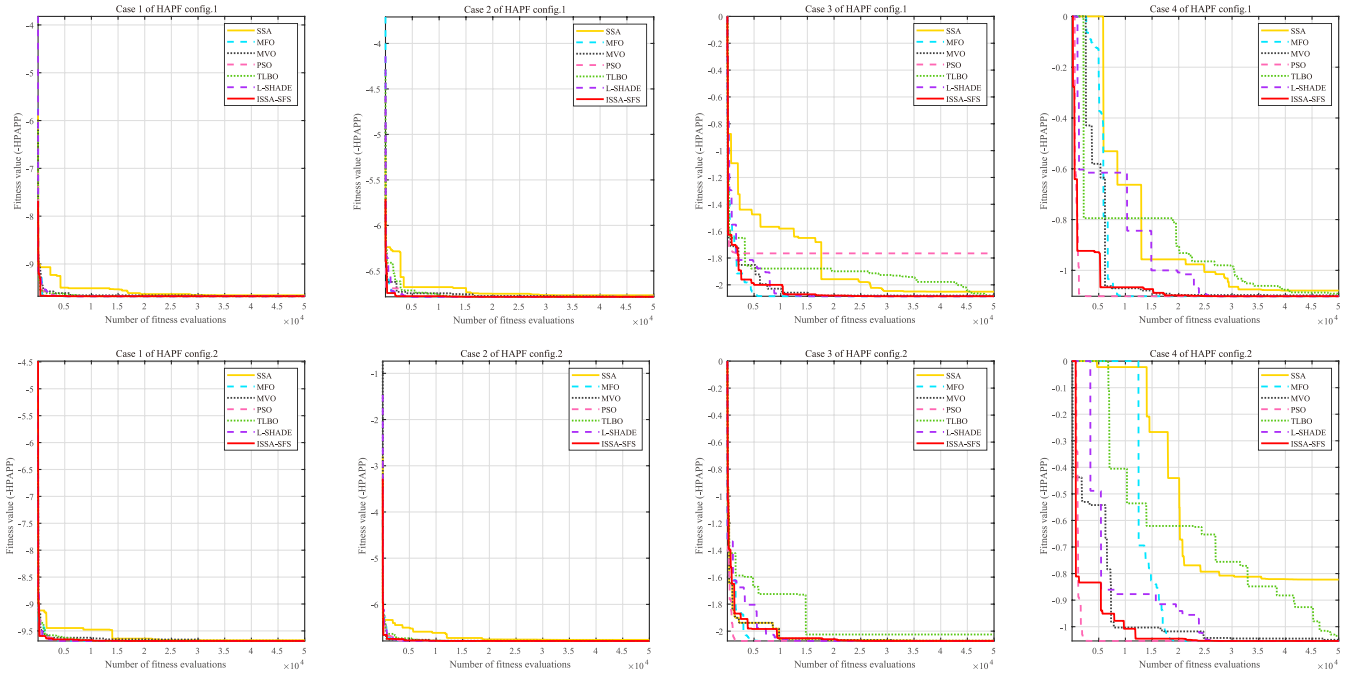

FIGURE 10. Convergence curves of all algorithms in study cases.

leader (ML) strategy, and the random learning (RL) strategy. Particularly, different from ISSA-SFS that combines three strategies, the ISSA-SFS-1 combines the ML strategy and the RL strategy, the ISSA-SFS-2 combines the SFS strategy and the RL strategy, and the ISSA-SFS-3 combines the SFS strategy and the ML strategy. The update processes of the mentioned algorithms are summarized and listed in Table 7. Additionally, their experimental results, the rank of mean values are also illustrated in Table 7. Note that the parameter setting and other conditions are the same as the preceding experiments. Furthermore, the average rank (i.e., the average of the ranks corresponding to the eight cases) and the final rank on all cases of HAPF configurations are listed in Table 8.

TABLE 8. Rankings of ISSA-SFS and its variants.

Algorithm	Average Rank	Final Rank
ISSA-SFS-1	3.13	3
ISSA-SFS-2	3.13	3
ISSA-SFS-3	2.63	2
ISSA-SFS	**1.13**	**1**

From Tables 7 and 8, ISSA-SFS can be seen to achieve the best or second-best results for most cases. In terms of all criteria, ISSA-SFS is superior to ISSA-SFS-1, ISSA-SFS-2, and ISSA-SFS-3. The satisfactory results indicate that the combination of the three different strategies dramatically improves the performance of ISSA-SFS.

As for the three ISSA-SFS variants, their results are all worse than ISSA-SFS, which means the three strategies are beneficial to seek out the optimal solution. In summary, all three new strategies are indispensable, removing any strategy is inadequate to achieve promising results, but integrating them will lead to excellent performance. The superior performance of ISSA-SFS confirms the appropriate balance between exploration and exploitation capability indeed benefits from the three strategies introduced by this research.

From the above experimental analysis, the accuracy and robustness of ISSA-SFS are verified. In order to analyze the superiority of ISSA-SFS further, the convergence curves of each comparison algorithm on the best value performance based on the 31 independent runs are described in Figure 10. Although PSO converges faster than ISSA-SFS in cases 3 and 4 of the two configurations, ISSA-SFS finds a smaller value than PSO. It is obviously seen that ISSA-SFS can achieve the best convergence characteristic among the mentioned seven algorithms in most study cases.

In conclusion, the above comparable results illustrated that the ISSA-SFS outperforms over the original SSA and other algorithms. Besides, the ISSA-SFS features superior searching accuracy, stronger robustness, and faster convergence speed when used to optimize the parameters of HAPF, its performance is confirmed to be satisfactory overall.

VI. CONCLUSION

The parameter identification of HAPF topologies is a complex multimodal issue involving numerous local optima, so it is very tricky for most existing algorithms to find the optimal global solution. To determine the optimal compensator parameters for HAPF configurations, we propose a novel application of an improved SSA called ISSA-SFS. The experimental results show that the proposed ISSA-SFS obtains the promising performance for recognizing the optimal

parameters of HAPF. The reason behind this fact that is given as follows. (1) In the ILP, the spiral flight search (SFS) strategy is used to improve the global search capability and avoid premature convergence. (2) In the ILP, a multiple leader (ML) strategy is developed to select multiple leaders for approaching the food source, which further improves the global search capability. (3) In the IFP, a simple random learning (RL) strategy is presented to learn two different random individuals, efficiently improving the local exploitation and accelerate the convergence speed. (4) By rationally combing the SFS strategy, the ML strategy, and the RL strategy with ILP and IFP, the proposed ISSA-SFS can effectively balance the exploitation and exploration perform in the entire iteration progress and find the optimal parameters of HAPF.

However, the proposed algorithm ISSA-SFS is relatively higher time consuming than SSA because of a sorting mechanism of salps in the ISSA-SFS. Therefore, the ISSA-SFS algorithm takes longer CPU time than the original SSA. In the future, we can conduct the sorting mechanism intermittently to decrease the computational of the sorting mechanism in each iteration. Furthermore, the new strategies from other meta-heuristic algorithms can be introduced into the proposed ISSA-SFS to replace the three proposed strategies of the ISSA-SFS and further improve the performance. In addition, the ISSA-SFS will be applied for optimizing the renewable energy system, photovoltaic cells system, and power point tracking issues.

REFERENCES

[1] Y.-J. Wang, R. M. O'Connell, and G. Brownfield, "Modeling and prediction of distribution system voltage distortion caused by nonlinear residential loads," *IEEE Trans. Power Del.*, vol. 16, no. 4, pp. 744–751, 2001.

[2] I. Rendroyoko and M. Rusli, "Development of power quality control procedures and standards to control the connection of non-linear loads in electric power systems," in *Proc. 22nd Int. Conf. Exhib. Electr. Distrib.*, Jun. 2013, pp. 1–6.

[3] R. Kingston and Y. Baghzouz, "Power factor and harmonic compensation in industrial power systems with nonlinear loads," in *Proc. Ind. Commercial Power Syst. Conf.*, May 1994, pp. 235–239.

[4] R. K. Garg, S. Ray, and N. Gupta, "Reactive power compensation and power factor improvement using fast active switching technique," in *Proc. IEEE 1st Int. Conf. Power Electron., Intell. Control Energy Syst. (ICPEICES)*, Jul. 2016, pp. 1–5.

[5] A. Hamadi, S. Rahmani, and K. Al-Haddad, "A novel hybrid series active filter for power quality compensation," in *Proc. IEEE Power Electron. Specialists Conf.*, Jun. 2007, pp. 1099–1104.

[6] B.-R. Lin, B.-R. Yang, and H.-R. Tsai, "Analysis and operation of hybrid active filter for harmonic elimination," *Electric Power Syst. Res.*, vol. 62, no. 3, pp. 191–200, Jul. 2002.

[7] I. Aminoroaya, H. R. Karshenas, A. Bakhshai, and P. Jain, "Converter rating reduction in hybrid active power filters (HAPF)," in *Proc. IEEE Energy Convers. Congr. Expo.*, Sep. 2011, pp. 1113–1118.

[8] C.-S. Lam, M.-C. Wong, W.-H. Choi, X.-X. Cui, H.-M. Mei, and J.-Z. Liu, "Design and performance of an adaptive Low-DC-Voltage-Controlled LC-hybrid active power filter with a neutral inductor in three-phase four-wire power systems," *IEEE Trans. Ind. Electron.*, vol. 61, no. 6, pp. 2635–2647, Jun. 2014.

[9] A. F. Zobaa and S. H. E. A. Aleem, "A new approach for harmonic distortion minimization in power systems supplying nonlinear loads," *IEEE Trans. Ind. Informat.*, vol. 10, no. 2, pp. 1401–1412, May 2014.

[10] A. Bhattacharya, C. Chakraborty, and S. Bhattacharya, "Parallel-connected shunt hybrid active power filters operating at different switching frequencies for improved performance," *IEEE Trans. Ind. Electron.*, vol. 59, no. 11, pp. 4007–4019, Nov. 2012.

[11] P. P. Biswas, P. N. Suganthan, and G. A. J. Amaratunga, "Minimizing harmonic distortion in power system with optimal design of hybrid active power filter using differential evolution," *Appl. Soft Comput.*, vol. 61, pp. 486–496, Dec. 2017.

[12] Z. Yan, C. Li, Z. Song, L. Xiong, and C. Luo, "An improved brain storming optimization algorithm for estimating parameters of photovoltaic models," *IEEE Access*, vol. 7, pp. 77629–77641, 2019.

[13] C. Li, Z. Song, J. Fan, Q. Cheng, and P. X. Liu, "A brain storm optimization with multi-information interactions for global optimization problems," *IEEE Access*, vol. 6, pp. 19304–19323, 2018.

[14] F. Olivas, F. Valdez, P. Melin, A. Sombra, and O. Castillo, "Interval type-2 fuzzy logic for dynamic parameter adaptation in a modified gravitational search algorithm," *Inf. Sci.*, vol. 476, pp. 159–175, Feb. 2019.

[15] P. Ochoa, O. Castillo, and J. Soria, "Optimization of fuzzy controller design using a differential evolution algorithm with dynamic parameter adaptation based on Type-1 and interval Type-2 fuzzy systems," *Soft Comput.*, vol. 24, no. 1, pp. 193–214, Jan. 2020.

[16] O. Castillo, L. Amador-Angulo, J. R. Castro, and M. Garcia-Valdez, "A comparative study of type-1 fuzzy logic systems, interval type-2 fuzzy logic systems and generalized type-2 fuzzy logic systems in control problems," *Inf. Sci.*, vol. 354, pp. 257–274, Aug. 2016.

[17] K. Yu, J. J. Liang, B. Y. Qu, Z. Cheng, and H. Wang, "Multiple learning backtracking search algorithm for estimating parameters of photovoltaic models," *Appl. Energy*, vol. 226, pp. 408–422, Sep. 2018.

[18] S. Mirjalili, A. H. Gandomi, S. Z. Mirjalili, S. Saremi, H. Faris, and S. M. Mirjalili, "Salp swarm algorithm: A bio-inspired optimizer for engineering design problems," *Adv. Eng. Softw.*, vol. 114, pp. 163–191, Dec. 2017.

[19] M. Abd Elaziz, A. A. Ewees, and Z. Alameer, "Improving adaptive neuro-fuzzy inference system based on a modified salp swarm algorithm using genetic algorithm to forecast crude oil price," *Natural Resour. Res.*, vol. 26, pp. 2671–2686, Nov. 2019.

[20] S. Kirkpatrick, C. D. Gelatt, and M. P. Vecchi, "Optimization by simulated annealing," *Science*, vol. 220, no. 4598, pp. 671–680, 1983.

[21] L. Davis, "Bit-climbing, representational bias, and test suit design," in *Proc. Int. Conf. Genetic Algorithm*, 1991, pp. 18–23.

[22] S. Mirjalili, S. M. Mirjalili, and A. Lewis, "Grey wolf optimizer," *Adv. Eng. Softw.*, vol. 69, pp. 46–61, Mar. 2014.

[23] S. Asaithambi and M. Rajappa, "Swarm intelligence-based approach for optimal design of CMOS differential amplifier and comparator circuit using a hybrid salp swarm algorithm," *Rev. Sci. Instrum.*, vol. 89, no. 5, May 2018, Art. no. 054702.

[24] J. Kennedy and R. Eberhart, "Particle swarm optimization," in *Proc. Int. Conf. Neural Netw. (ICNN)*, Nov./Dec. 1995, pp. 1942–1948.

[25] H. Faris, M. M. Mafarja, A. A. Heidari, I. Aljarah, A. M. Al-Zoubi, S. Mirjalili, and H. Fujita, "An efficient binary salp swarm algorithm with crossover scheme for feature selection problems," *Knowl.-Based Syst.*, vol. 154, pp. 43–67, Aug. 2018.

[26] K. G. Dhal, S. Ray, A. Das, and S. Das, "A survey on nature-inspired optimization algorithms and their application in image enhancement domain," *Arch. Comput. Methods Eng.*, vol. 26, no. 5, pp. 1607–1638, Nov. 2019.

[27] A. A. El-Fergany, "Extracting optimal parameters of PEM fuel cells using salp swarm optimizer," *Renew. Energy*, vol. 119, pp. 641–648, Apr. 2018.

[28] L. Abualigah, M. Shehab, M. Alshinwan, and H. Alabool, "Salp swarm algorithm: A comprehensive survey," *Neural Comput. Appl.*, vol. 32, no. 15, pp. 11195–11215, Aug. 2020.

[29] N. Singh, L. H. Son, F. Chiclana, and J.-P. Magnot, "A new fusion of salp swarm with sine cosine for optimization of non-linear functions," *Eng. with Comput.*, vol. 36, no. 1, pp. 185–212, Jan. 2020.

[30] A. E. Hegazy, M. A. Makhlouf, and G. S. El-Tawel, "Improved salp swarm algorithm for feature selection," *J. King Saud Univ.-Comput. Inf. Sci.*, vol. 32, no. 3, pp. 335–344, Mar. 2020.

[31] G. I. Sayed, G. Khoriba, and M. H. Haggag, "A novel chaotic salp swarm algorithm for global optimization and feature selection," *Int. J. Speech Technol.*, vol. 48, no. 10, pp. 3462–3481, Oct. 2018.

[32] M. H. Qais, H. M. Hasanien, and S. Alghuwainem, "Enhanced salp swarm algorithm: Application to variable speed wind generators," *Eng. Appl. Artif. Intell.*, vol. 80, pp. 82–96, Apr. 2019.

[33] D. H. Wolpert and W. G. Macready, "No free lunch theorems for optimization," *IEEE Trans. Evol. Comput.*, vol. 1, no. 1, pp. 67–82, Apr. 1997.

[34] S. Mirjalili, "Moth-flame optimization algorithm: A novel nature-inspired heuristic paradigm," *Knowl.-Based Syst.*, vol. 89, pp. 228–249, Nov. 2015.
[35] R. V. Rao, V. J. Savsani, and D. P. Vakharia, "Teaching–learning-based optimization: A novel method for constrained mechanical design optimization problems," *Comput.-Aided Des.*, vol. 43, no. 3, pp. 303–315, Mar. 2011.
[36] S. Mirjalili, S. M. Mirjalili, and A. Hatamlou, "Multi-verse optimizer: A nature-inspired algorithm for global optimization," *Neural Comput. Appl.*, vol. 27, no. 2, pp. 495–513, Feb. 2016.
[37] L. Gyugyi, "Active ac power filter," in *Proc. IEEE/IAS Annu. Meeting*, Oct. 1976, pp. 529–535.
[38] F. Z. Peng, H. Akagi, and A. Nabae, "A new approach to harmonic compensation in power systems-a combined system of shunt passive and series active filters," *IEEE Trans. Ind. Appl.*, vol. 26, no. 6, pp. 983–990, Nov./Dec. 1990.
[39] H. Fujita and H. Akagi, "A practical approach to harmonic compensation in power systems-series connection of passive and active filters," *IEEE Trans. Ind. Appl.*, vol. 27, no. 6, pp. 1020–1025, Nov./Dec. 1991.
[40] F. Z. Peng, "Harmonic sources and filtering approaches," *IEEE Ind. Appl. Mag.*, vol. 7, no. 4, pp. 18–25, Jul./Aug. 2001.
[41] S. Rahmani, A. Hamadi, and K. Al-Haddad, "A comprehensive analysis of hybrid active power filter for power quality enhancement," in *Proc. 38th Annu. Conf. IEEE Ind. Electron. Soc. (IECON)*, Oct. 2012, pp. 6258–6267.
[42] A. F. Zobaa, "Optimal multiobjective design of hybrid active power filters considering a distorted environment," *IEEE Trans. Ind. Electron.*, vol. 61, no. 1, pp. 107–114, Jan. 2014.
[43] R. Langella and A. Testa, *IEEE Standard Definitions for the Measurement of Electric Power Quantities Under Sinusoidal, Nonsinusoidal, Balanced, or Unbalanced Conditions*, IEEE Standard 1459-2010 (Revision of IEEE std 1459-2000), 2010.
[44] *IEEE Recommended Practice and Requirements for Harmonic Control in Electric Power Systems*, IEEE Standard 519-2014 (Revision of IEEE Standard 519-1992), 2014.
[45] W. Wong and C. I. Ming, "A review on Metaheuristic algorithms: Recent trends, benchmarking and applications," in *Proc. 7th Int. Conf. Smart Comput. Commun. (ICSCC)*, Jun. 2019, pp. 1–5.
[46] D. E. Goldberg and J. H. Holland, "Genetic algorithms and machine learning," *Mach. Learn.*, vol. 3, no. 2, pp. 95–99, Oct. 1988.
[47] R. Storn and K. Price, "Differential evolution-a simple and efficient heuristic for global optimization over continuous spaces," *J. Global Optim.*, vol. 11, no. 4, pp. 341–359, 1997.
[48] D. Karaboga and B. Basturk, "Artificial bee colony (ABC) optimization algorithm for solving constrained optimization problems," in *Proc. Found. Fuzzy Log. Soft Comput.* Berlin, Germany: Springer, 2007, pp. 789–798.
[49] S. Saremi, S. Mirjalili, and A. Lewis, "Grasshopper optimisation algorithm: Theory and application," *Adv. Eng. Softw.*, vol. 105, pp. 30–47, Mar. 2017.
[50] *IEEE Recommended Practice and Requirements for Harmonic Control in Electric Power Systems*. New York, NY, USA: IEEE Press, Jun. 2014, pp. 1–29.
[51] J. Derrac, S. García, D. Molina, and F. Herrera, "A practical tutorial on the use of nonparametric statistical tests as a methodology for comparing evolutionary and swarm intelligence algorithms," *Swarm Evol. Comput.*, vol. 1, no. 1, pp. 3–18, Mar. 2011.